

# Characterizing a Cold Gas Thruster System

Max Huggins – UCA Department of Physics and Astronomy

April 28, 2020

## Abstract

A cold gas thruster (CGT) system was designed with pre-existing nozzle theory in mind. This paper deals with characterizing the system and provides an analysis of the force production for it. It was found that the CGT performed similarly to the predicted theory, but the data collected was not sufficient to characterize the system as was previously expected. Changes must be made to the experimental setup to complete the characterization.

## Nomenclature

$\epsilon$	Area expansion ratio for nozzle
$\gamma$	Ratio of specific heats
$\rho_c$	Density at chamber temperature and pressure
$\tau$	Time of full trial
$A_e$	Exit area of nozzle
$A_t$	Throat area of nozzle
$C_F$	Thrust coefficient
$F$	Force or thrust
$g$	Acceleration due to gravity
$I_{sp}$	Specific impulse
$M$	Mach number
$m$	Mass
$N1$	No expansion, trial 1
$N2$	No expansion, trial 2

$O1$	Optimum area ratio, trial 1
$O11$	Overexpanded area ratio 1, trial 1
$O12$	Overexpanded area ratio 1, trial 2
$O2$	Optimum area ratio, trial 2
$O21$	Overexpanded area ratio 2, trial 1
$O22$	Overexpanded area ratio 2, trial 2
$O31$	Overexpanded area ratio 3, trial 1
$O32$	Overexpanded area ratio 3, trial 2
$O41$	Overexpanded area ratio 4, trial 1
$O42$	Overexpanded area ratio 4, trial 2
$P_a$	Ambient pressure
$P_c$	Chamber pressure
$P_e$	Exit pressure
$R$	Universal gas constant
$t$	Time
$T_c$	Chamber temperature
$T_e$	Exit temperature
$U11$	Underexpanded area ratio 1, trial 1
$U12$	Underexpanded area ratio 1, trial 2
$U21$	Underexpanded area ratio 2, trial 1
$U22$	Underexpanded area ratio 2, trial 2
$U31$	Underexpanded area ratio 3, trial 1
$U32$	Underexpanded area ratio 3, trial 2
$U41$	Underexpanded area ratio 4, trial 1
$U42$	Underexpanded area ratio 4, trial 2
$v$	Gas velocity
$W$	Molecular weight of the gas
$w$	Mass flow rate
$X_x$	Any variable, X at some point, x

# 1 Introduction

A cold gas thruster (CGT) is a system that uses expanding gas to generate a force. This force is typically used in reaction control systems (RCSs) to stabilize space craft or simply change their attitude. This paper is primarily concerned with reaction control systems to be developed for high altitude balloon payloads (HABPs.) These HABPs experience intense and sporadic winds. Winds which make data collection for certain sensors difficult. There are several ways in which a RCS can achieve stabilization, but the method of choice here is the CGT.

There are several components important to the CGT RCS. Here, there will only be a brief discussion on two of these components such that the analysis is not lacking information.

The first consideration to make is the type of gas to be used. The primary question here is, *what makes one gas better than another?* One parameter that tries to answer this question is the *specific impulse* ( $I_{sp}$ ). This is a value specific to a gas. Experimentally, it is measured by integrating a force (F) versus time (t) plot generated by a CGT using that gas. That will give the total impulse, this is divided by the change in weight of the gas through that time period ( $\tau$ ). In other words:

$$I_{sp} = \frac{\sum_{t=0}^{\tau} F(t)t}{\Delta mg} \quad (1)$$

where  $\Delta m$  is mass and  $g$  is acceleration due to gravity. More precisely, specific impulse is defined by equation 2.

$$I_{sp} = \frac{F}{dm/dt} \quad (2)$$

You may notice the discrepancy in units between equations 1 and 2. Often times the  $I_{sp}$  is given with units of s, but in reality it is defined with units of  $Ns/kg$ . Additionally, the theoretical value is given by reference [2] and is shown in equation 3.

$$I_{sp} = \left[ \frac{2\gamma RT_c}{(\gamma - 1)W} \left( 1 - \left( \frac{P_e}{P_c} \right)^{\frac{\gamma-1}{\gamma}} \right) \right]^{\frac{1}{2}} + \frac{(P_e - P_a) A_e}{P_c} \frac{1}{A_t C_D} \quad (3)$$

where  $C_D$  is the discharge coefficient and is defined by equation 4.

$$C_D = \sqrt{\frac{\gamma \rho_c}{P_c}} \left( \frac{2}{\gamma + 1} \right)^{\frac{\gamma+1}{2(\gamma-1)}} \quad (4)$$

The same dependencies seen here, are also seen in the force equation. This is an excellent start to creating a standard for comparing gases, but there is much more that should be considered. Factors such as safety, availability, cost, energy storage density, and so on all contribute to the choice of gas. Additionally, each one of these factors has a different weight per say depending on the scenario in which they are being applied. After consideration, the choice of gas for this system is  $CO_2$ .

The other component is the nozzle. These are used to set the mass flow rate for the system and to accelerate the propellant to supersonic speeds. They consist of a converging section that leads into a throat of minimum radius and a diverging section. Figure 1 shows a simple

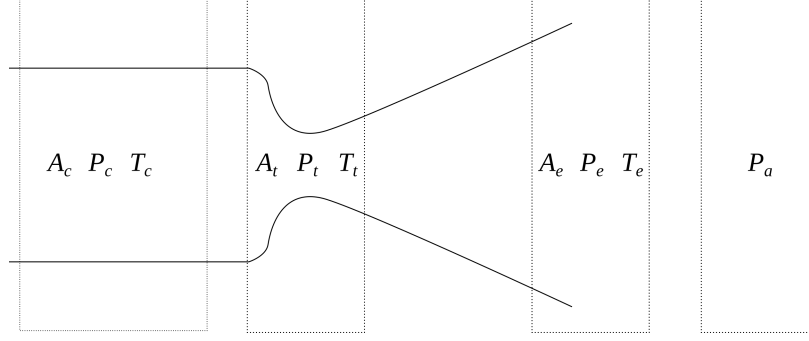


Figure 1: Simple nozzle cross-section showing four regions of interest

2D section of a typical nozzle. The four regions of this nozzle are the chamber (c), throat (t), exit (e), and ambient (a). Some variables of interest are shown for each region.

Nozzles that have been made to achieve maximum thrust obey the following characteristics. In the converging section, the gas is accelerated; once the throat is reached the gas is traveling at the speed of sound. Then, as it proceeds into the diverging section, it continues to accelerate until it reaches the exit plane of the nozzle. Ideally, the nozzle is designed such that the pressure of the gas exiting the nozzle is equal to the ambient pressure.

The thrust produced by a nozzle can be written in terms of the variables listed below. First, though, it is given by equation 5 in reference [2].

- Chamber Temperature ( $T_c$ )
- Exit Temperature ( $T_e$ )
- Chamber Pressure ( $P_c$ )
- Exit Area of Nozzle ( $A_e$ )
- Throat Area of Nozzle ( $A_t$ )

The derivation will not be shown here, but reference [2] discusses it in detail. The text derives equation 5 from the laws of thermodynamics and some general assumptions.

$$C_F = \sqrt{\frac{2\gamma^2}{\gamma-1} \left(\frac{2}{\gamma+1}\right)^{\frac{\gamma+1}{\gamma-1}} \left(1 - \left(\frac{P_e}{P_c}\right)^{\frac{\gamma-1}{\gamma}}\right)} + \frac{(P_e - P_a) A_e}{P_c A_t} \quad (5)$$

Where  $C_F$  is defined by:

$$C_F = \frac{F}{A_t P_c} \quad (6)$$

It is also helpful to define the nozzle's expansion ratio ( $\epsilon$ ), given by equation 7.

$$\epsilon = \frac{A_e}{A_t} \quad (7)$$

It can be seen  $C_F$ , ergo the thrust, is at maximum when  $P_a = P_e = 0$ . It is also shown that  $\frac{P_e}{P_c}$  is given by equation 8.

$$\frac{P_e}{P_c} = \left(1 + \frac{(\gamma - 1)}{2} M^2\right)^{\frac{\gamma}{\gamma - 1}} \quad (8)$$

Additionally, we can define the mach number as:

$$M^2 = \frac{2}{\gamma - 1} \left(\frac{T_c}{T_e} - 1\right) \quad (9)$$

allowing us to make a substitution for  $\frac{P_e}{P_c}$  into equation 5. With this substitution, we will eliminate  $P_e$ . The motivation for this is that measuring the exit plane pressure is more difficult than measuring the exit plane temperature. After the substitutions, we retrieve equation 10.

$$F = A_t P_c \left( \sqrt{\frac{2\gamma^2}{\gamma - 1} \left(\frac{2}{\gamma + 1}\right)^{\frac{\gamma + 1}{\gamma - 1}} \left(1 - \frac{T_e}{T_c}\right)} + \left( \left(\frac{T_e}{T_c}\right)^{\frac{\gamma}{\gamma - 1}} - \frac{P_a}{P_c} \right) \epsilon \right) \quad (10)$$

This equation was developed given some assumptions and in different systems some of the assumptions may have a more or less dominant effect. It can also be seen that since the thrust is highly dependent on the external pressure, the nozzle should be designed to maximize the thrust in the pressure it will spend the most time in. Because of this an experiment was developed to determine the reliability of equation 10. Using similar methods, equation 3 can be expressed in terms of relevant variables as shown in equation 11.

$$I_{sp} = \left[ \frac{2\gamma R T_c}{W(\gamma - 1)} \left(1 - \frac{T_e}{T_c}\right) \right]^{\frac{1}{2}} + \left[ \left(\frac{T_e}{T_c}\right)^{\frac{\gamma}{\gamma - 1}} - \frac{P_a}{P_c} \right] \frac{A_e}{A_t} \sqrt{\frac{P_c}{\gamma \rho_c}} \left(\frac{\gamma + 1}{2}\right)^{\frac{\gamma + 1}{2(\gamma - 1)}} \quad (11)$$

In measuring the thrust at several different area ratios and comparing it to the predicted thrust, the hope is to create an "effective" proportionality constant for the specific impulse. This would then allow the nozzle design process to be maximized for pressures that cannot be tested on Earth's surface.

## 2 Data Collection and Analysis

### 2.1 Data Collection

The data taken was for the variables in equation 10. There were a total of 10 nozzle expansion ratios used with 2 trials each. The expansion ratio kept  $A_t$  constant and varied  $A_e$ . There were 4 over expanded, 4 underexpanded, 1 optimum, and 1 with no expansion. The naming scheme goes something like ERT, where E stands for either U (Underexpanded), N (None), or O. O stands for either optimum or overexpanded. R is the ratio number (1-4) except in the case that there is no third character. In this case the O stands for optimum, which there is only one of. T stands for trial number which can be either 1 or 2. So for example, U22 is underexpanded, ratio number 2, trial number 2. O1 is optimum ratio, trial number 1. These are explicitly defined in the nomenclature section. This naming scheme will be upated in future experiments because it was slightly problematic in the analysis of the data.

## Data Sensors

There should be some light discussion on the sensors used for data collection. There was a single pressure transducer located near the inlet of the nozzle, a thermocouple located on the nozzle, a thermocouple located inside of the adaptor that the  $CO_2$  connected to the rest of the plumbing, and a load cell setup to measure the thrust produced from the CGT. For sake of simplicity I will refer to these as "sensors" preceded by the variable they measured. So, respectively,  $P_c$  sensor,  $T_e$  sensor,  $T_c$  sensor, and  $F$  sensor. Additionally,  $\gamma$  is dependent on temperature, but only changes slightly in the temperature differences noticed here. In later models,  $\gamma$  will be set to be a function of temperature for greater accuracy. For now it is not necessary because the force has a small dependence on  $\gamma$  compared to the temperature. So, for the sake of this project  $\gamma$  is a constant. The data acquisition system was running python on a RaspberryPi 3 and since all of these sensors are analog devices 2 different analog-to-digital converters (ADCs) was used to interface with the Pi. The  $P_c$ ,  $T_e$ , and  $T_c$  sensors interfaced with a 10-bit ADC and the  $F$  sensor interfaced with a 24-bit ADC. In future experiments, a 24-bit ADC will be used for all data acquisition because of the limited resolution with the 10-bit ADC. This is especially evident with the thermocouple data. All of the python scripts for data collection are available at my [GitHub repository](#).

The code began the experiment after all sensors were calibrated and functioning properly. Data collection ran until the force production was below a certain threshold for a predefined number of points. This would also need to be updated because often times the force sensor would lose its zero position so defining the threshold value was not so easy. A better method would be using the change in force to determine when the experiment was over. This would work well because the force is transient until the  $CO_2$  was all spent. After it was over the mass of the  $CO_2$  canister was measured. All of this data was written to two separate .txt files. One included the calibration values for the sensors and changes in mass, the other included  $P_c$ ,  $T_c$ ,  $T_e$ , and  $F$ . The previous was not recorded in a useful format and later work had to be done to resolve this. In the future this should be updated. The latter was simply comma delimited and worked fine for reading into python for analysis. The data files can be found at this [GitHub repository](#) as well.

## 2.2 Initial Analysis

To begin the analysis, simple plots were made to look at the sensor data over time. Immediately, it was found that the temperature data is quite poor! The resolution of the ADC is evident in the discrete steps that the temperature takes. Figure 2 shows an example of the temperature data. The limited resolution of the ADC can be seen quite clearly. However, this is not terribly problematic and several things can be done to smooth the curve. Since smoothing this data is not the objective here, I have simply taken a function from the pandas python library that handles smoothing quite well. It uses a moving averages method. The smoothed plot is shown in figure 3. There are additional problems that come with smoothing data, though. The total number of points is typically reduced and therefore all of the data that is going to be used must then be smoothed by the same factor. Also, the data is shifted

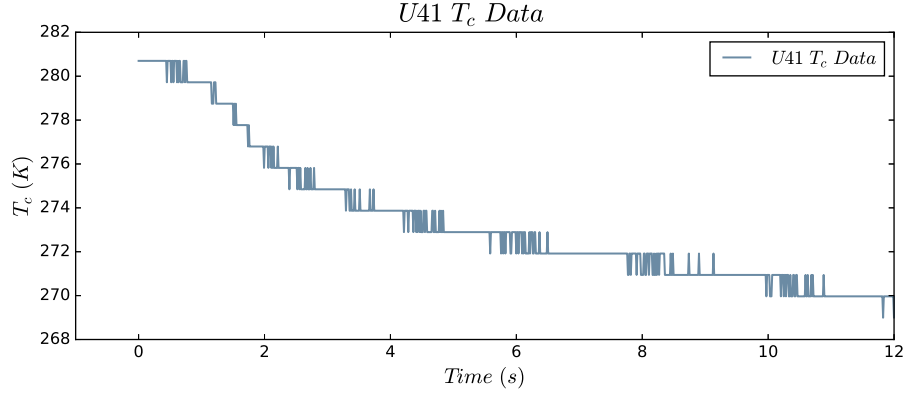


Figure 2: Example plot of the temperature over time for a trial

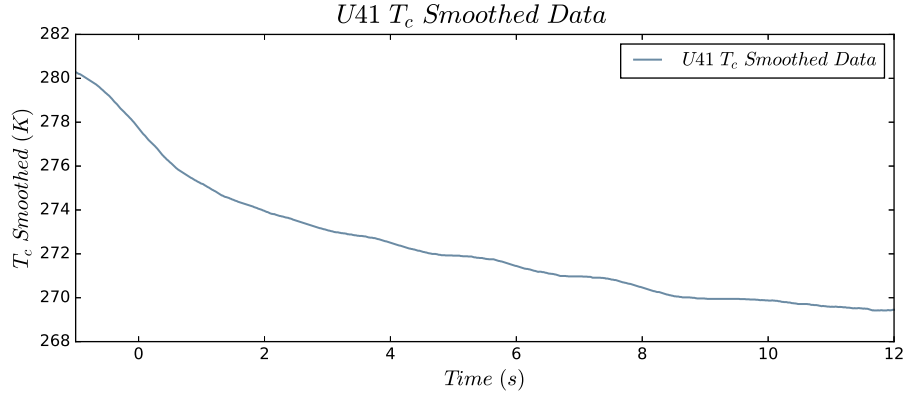


Figure 3: Example plot now smoothed

to the left as can be seen from figures 2 and 3. Alternatively, a function could be fit to the data and this would allow the possibility of a continuous data set. For now though, there are bigger problems with the data recorded. Figure 4 shows the two different temperature data sets plotted against time for one of the trials. It can be seen immediately that at some point

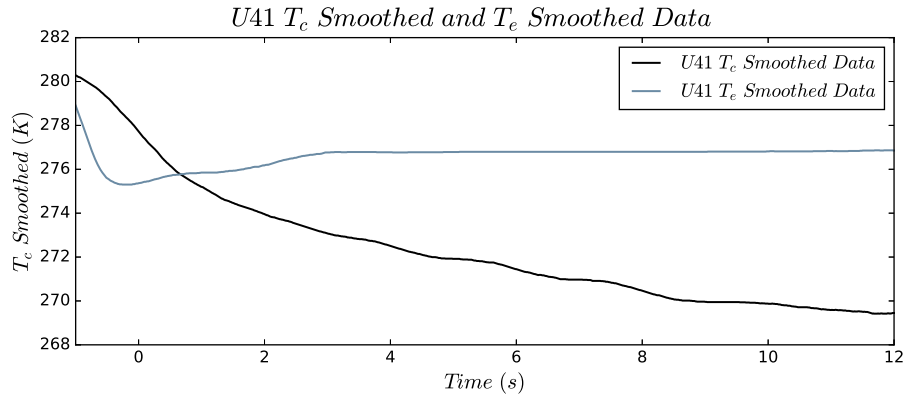


Figure 4: Smoothed  $T_c$  and  $T_e$  plotted with time for one of the trials

the  $T_c$  line drops below the  $T_e$  line. Looking back at equation 10 this is troublesome. This means that  $\left(1 - \frac{T_e}{T_c}\right) < 0$  giving an overall negative sign under the square root. Obviously the force produced is not imaginary, so either the data collected for these temperatures is not representative of the actual variables or the theory is wrong. It is obvious that the former is the problem for several reasons. The first is that the  $T_c$  variable represents the temperature directly before the converging section of the nozzle.  $T_e$  is the temperature of the exit plane of the nozzle. The two thermocouples are not placed in these regions. Admittadely, there was not enough attention when inspecting the theory to develop the experiment. Under normal circumstances some simple changes would be made and new data would be taken, however due to the closure of the university nothing can be done about collecting new data. Because of this we will proceed with what analysis can be completed and use a more general approach to characterizing the CGT. First, I've plotted the predicted force with the experimental force in figure 5. As expected, we see segments where the force is undefined due to a runtime error

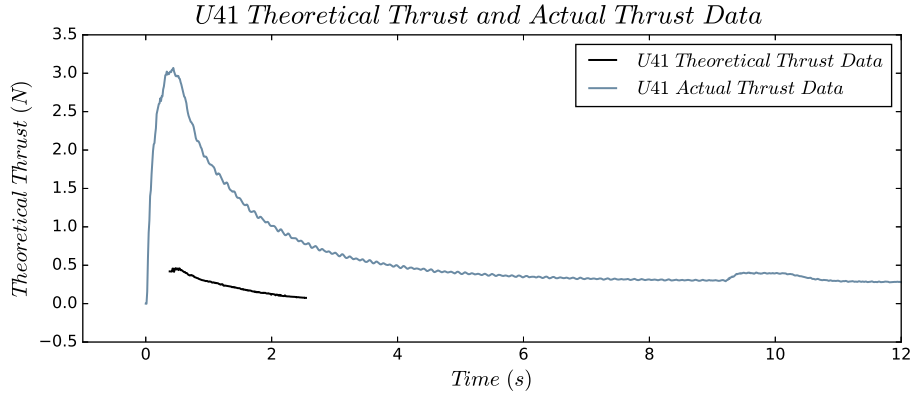


Figure 5: First attempt at plotting the thrust and predicted thrust against time

in the numpy package. What can be done here? Well, some more consideration should be taken into the theory. Starting with a gas obeying the ideal gas law in an adiabatic system.

$$P_x V_x = nRT_x \quad (12)$$

where x is some point along the nozzle's axial direction.

$$P_x V_x^\gamma = P_{x+dx} V_{x+dx}^\gamma \quad (13)$$

after some substitution we can obtain 14.

$$\left(\frac{P_x}{P_{x+dx}}\right)^{\frac{\gamma-1}{\gamma}} = \frac{T_x}{T_{x+dx}} \quad (14)$$

now, if  $P_x = P_c$  and  $P_{x+dx} = P_e$ , we can look at this negative sign more intuitively. We know that a nozzle will never function properly in a state where the exit plane pressure is less than the chamber pressure. Also, since the  $\gamma$  value is always greater than 1, the overall term will be greater than 1 which means the exit plane temperature must always be less than the



chamber temperature. In other words, we know  $P_c > P_e$  and  $\gamma > 1$  therefore,  $\left(\frac{P_c}{P_e}\right)^{\frac{\gamma-1}{\gamma}} > 1$  which also means  $T_c > T_e$  always. Additionally, since gases cool as they expand, it is sensible that the chamber will be warmer than the exit plane of the nozzle.

At this point, confidence has been established in the theory and changes should be made to the experimental setup. Again, unfortunately, these changes cannot be made but we will continue with the analysis regardless.

## 2.3 Attempt at Reconciliation

The most obvious way to resolve the negative sign is to include an absolute value around the problematic term. This solves the runtime error, but is unfounded. We know the optimum nozzle expansion ratio should have the largest thrust production, but we have essentially removed  $T_e$ 's dependence on the expansion ratio in doing this. This means the thrust will be highest for the value which has the greatest expansion ratio which is geometry O4. This can be seen in figure 6. I have plotted several trials there and included the predicted force according to equation 10. O4 is indeed the largest thrust curve. Also, in viewing these thrust

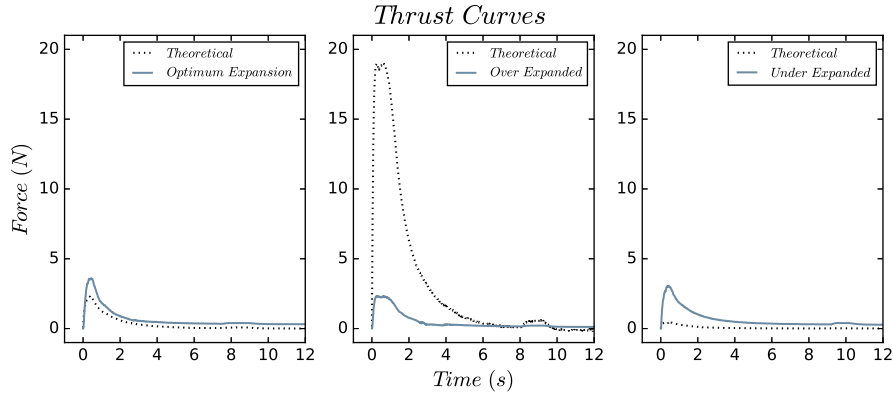


Figure 6: Several trials thrust curves plotted with the predicted thrust

curves it is important to recognize the predicted force is the predicted force per unit mass, but the actual curve is per some different mass value. However, the unit for the mass can be set to some convenient unit and be compared through all the data. This won't change the actual analysis and design conditions.

Tacking on an absolute value will not only fail to resolve the issue here but it is also unfounded. The next thought is to solve for  $T_e$  in terms of the other available variables. It turns out that  $T_e$  can be put in terms of  $T_c$ ,  $P_c$ ,  $A_e$ ,  $\rho_c$ , and  $w$ . Unfortunately, there are several problems with this. The first is that the change in mass, the mass flow rate, was only measured as an initial and final value. Meaning the total mass used throughout the experiment is known, but the mass flow rate throughout is not. For now, the assumption will be made that the mass flow rate is constant. Next, as can be seen from equation 15  $T_e$  cannot be solved algebraically.

It is not difficult to solve for it computationally though.

$$T_e = T_c \left[ \frac{\gamma - 1}{2\gamma P_c \rho_c} \left( \frac{w}{A_e} \right)^2 \left( \frac{T_c}{T_e} \right)^{\frac{\gamma+1}{\gamma-1}} + 1 \right]^{-1} \quad (15)$$

The simplest method is to use the relaxation method as described in [3]. The process is to iterate the equation by plugging in  $T_e = 1$  on the right side, finding a new value for  $T_e$  on the left side, substituting this value back into the right side, and so on.  $T_e$  should converge to a value and that is the solution for  $T_e$ . Using this method, I've made the same plots in figure 7 as in figure 6. The similarity between the two figures is quite apparent. At first glance, they

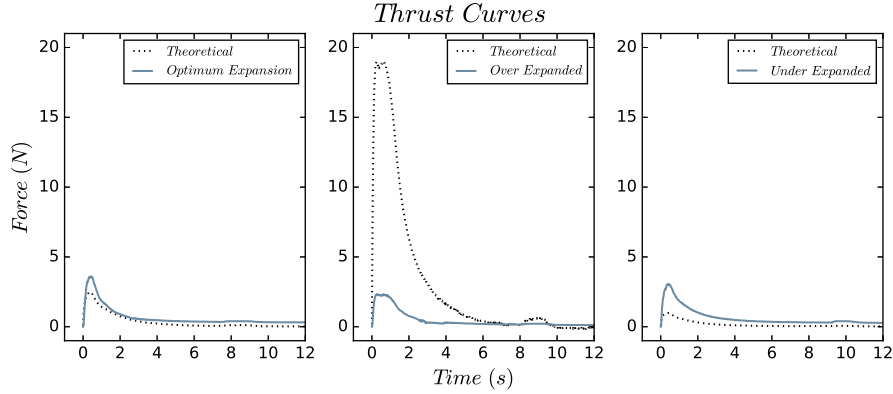


Figure 7: Several trials thrust curves plotted with the predicted thrust

nearly look the same, but looking at the far right plot the theoretical curve can be seen to be different from the other. The reason for this is because the assumption made about the mass flow rate being constant through time was naive. The mass flow rate, at any point  $x$  can be defined by equation 16.

$$w_x = A_x v_x \rho_x \quad (16)$$

Both the velocity and density of the gas have dependence on pressure and temperature so  $w$  is *not* constant with respect to time. That is not to say it is not constant at any given time throughout the entire system, however. If  $T_e$  is not represented correctly it is clear that the result is that the nozzle with the largest expansion ratio is predicted to function best because of equation 10's dependence on  $A_e$ .

In the end, there is not much reconciliation that can be done for the poor data collection. What we can look at effectively is the experimental value for the specific impulse. Unfortunately, this won't tell much because the theoretical values cannot be calculated for the same reasons as the force. Additionally, it is not ideal to look at the specific impulse over the entire experiment because the temperature and pressure are so transient. However, since the change in mass is only known for two data points it is the best that can be done. Determining these values is a simple trapezoidal sum over all time. I've tabulated all of these in table 1.

There isn't much to see here, except that the values found are close to the known values from reference [1]. The  $I'_{sp}$ 's dependence on temperature and pressure means that these values are meaningless without the theoretical values at the same pressure and temperature. Reference [1] is using values for the maximum possible  $I_{sp}$  values.

Geometry	<i>Trial 1</i> $I_{sp}$	<i>Trial 2</i> $I_{sp}$
N	61.1	54.0
U4	58.0	44.1
U3	33.5	52.8
U2	62.5	60.3
U1	33.9	62.6
O	57.5	37.3
O1	58.6	59.5
O2	50.5	48.3
O3	29.0	60.3
O4	44.6	56.0

Table 1: Experimental specific impulses

### 3 Results of Analysis

Unfortunately, the result of this analysis is not significant in terms of directly characterizing the CGT system. The goal was to compare theoretical force and specific impulse data with experimental force and specific impulse data. Obviously, this was not completed here. Plots have been made, different techniques have been used, and values have been found but none of them have much real significance without their theoretical counterparts. The primary value of the analysis performed above is the scripting. All of the scripting was done in python and is object oriented. This means that once the corrections have been made to the experimental apparatus, there is little to no work to be done in terms of analysis.

### 4 Conclusion

The data set used for this paper was taken with the purpose of characterizing the cold gas thruster system. This would be done with the use of existing nozzle theory that describes the specific impulse and force equations for a converging-diverging nozzle. The variables *meant* to be measured are  $P_c$ ,  $T_e$ ,  $T_c$ ,  $F$ , and  $w$  and with them this purpose could be achieved. However, the experimental setup does not represent them correctly. Namely, the  $T_e$  sensor is not placed correctly and  $w$  is not measured through time. The solutions here are straightforward.

The analysis has been done in an object oriented paradigm that allows for ease of analysis for future datasets. In the time that cannot be spent in the lab some changes can be made to the scripting. The code lacks efficiency and readability. Because of this changes should be made to follow a more standard coding scheme or style.

Again, all of this scripting and data is available at this [GitHub repository](#).

### References

- [1] Assad Anis. Cold gas propulsion system-an ideal choice for remote sensing small satellites. *Remote sensing-advanced techniques and platforms*, pages 447–462, 2012.

- [2] Norman Harry Langton. *Rocket propulsion*. Space research and technology: v. 2. American Elsevier Pub. Co., 1970.
- [3] Mark Newman. *Computational Physics*, volume 1. Mark Newman, 1 edition, 2012.